

# Membrane Protein Simulations Using AMBER Force Field and Berger Lipid Parameters

Arnau Cordoní,\* Gianluigi Caltabiano, and Leonardo Pardo

Laboratori de Medicina Computacional, Unitat de Bioestadística, Facultat de Medicina, Universitat Autònoma de Barcelona, 08193 Bellaterra, Spain

**ABSTRACT:** AMBER force fields are among the most commonly used in molecular dynamics (MD) simulations of proteins. Unfortunately, they lack a specific set of lipid parameters, thus limiting its use in membrane protein simulations. In order to overcome this limitation we assessed whether the widely used united-atom lipid parameters described by Berger and co-workers could be used in conjunction with AMBER force fields in simulations of membrane proteins. Thus, free energies of solvation in water and in cyclohexane, and free energies of water to cyclohexane transfer, were computed by thermodynamic integration procedures for neutral amino acid side-chains employing AMBER99, AMBER03, and OPLS-AA amino acid force fields. In addition, MD simulations of three membrane proteins in a POPC lipid bilayer, the  $\beta 2$  adrenergic G protein-coupled receptor, Aquaporin-1, and the outer membrane protein Omp32, were performed with the aim of comparing the AMBER99SB/Berger combination of force fields with the OPLS-AA/Berger combination. We have shown that AMBER99SB and Berger force fields are compatible, they provide reliable free energy estimations relative to experimental values, and their combination properly describes both membrane and protein structural properties. We then suggest that the AMBER99SB/Berger combination is a reliable choice for the simulation of membrane proteins, which links the easiness of ligand parametrization and the ability to reproduce secondary structure of AMBER99SB force field with the largely validated Berger lipid parameters.

## ■ INTRODUCTION

Molecular dynamics (MD) simulations is a widely used technique that has successfully been employed to yield novel insights in a huge variety of systems such as peptides, proteins, nucleic acids, drug-like molecules, solvents, gas-phases, and membranes.<sup>1,2</sup> Membrane proteins represent 30% of all proteins in sequenced genomes and account for 70% of drug targets,<sup>3</sup> but only 2% of crystal structures deposited in the Protein Data Bank are membrane proteins.<sup>4</sup> Thus, an important application of MD simulations is in the field of membrane proteins, due to the limited high-resolution structural information.<sup>5,6</sup> Attaining high-quality results requires, however, accurate force field parameters and a careful choice of the simulation conditions.<sup>7,8</sup> There are four commonly used biomolecular force fields: AMBER,<sup>9,10</sup> CHARMM,<sup>11,12</sup> OPLS-AA,<sup>13,14</sup> and GROMOS,<sup>15</sup> the first three being all-atom force fields and the last an united-atom force field (nonpolar hydrogens are treated as part of the adjacent carbon). Unfortunately, none of them is, in the present form, optimized to perform simulations of membrane proteins in complex with synthetic, drug-like ligands. Parameterization of ligands using OPLS-AA, CHARMM, or GROMOS force fields is not straightforward, while this task can easily be achieved within the AMBER force fields thanks to the generic General Amber Force Field (GAFF)<sup>16</sup> and ANTECHAMBER suite of programs.<sup>17</sup> AMBER force fields miss build-in parameters for lipids, although it is possible to simulate protein–lipid complexes by combining GLYCAM06<sup>18</sup> and AMBER. Both CHARMM and GROMOS force fields contain a specific set of parameters for lipids. Nonetheless, these parameters fail to correctly reproduce the membrane surface area if a surface tension is not applied.<sup>19</sup> This is a major problem in membrane

protein simulations since the magnitude of the surface tension is generally unknown. Recently reported simulations of lipid bilayers built on AMBER GAFF suffered from similar problems.<sup>20–22</sup> In an attempt to overcome this obstacle, new lipid parameters were reported that better reproduce the experimental surface areas without applying a surface tension within CHARMM<sup>19</sup> and GROMOS<sup>23</sup> force fields.

The lipid parameters of Berger and collaborators are united-atom parameters that correctly reproduce the structural features of phosphatidylcholine bilayers in a variety of systems including ions, cholesterol, peptides, and proteins,<sup>24–28</sup> without the need to apply any surface tension to the system. They were created on the basis of an early parametrization by Essex<sup>29</sup> developed from the united-atom OPLS (OPLS-UA) force field.<sup>13</sup> Berger and co-workers further optimized Lennard-Jones (LJ) parameters for lipid tails to best reproduce thermodynamic experimental data of pentadecane. Since OPLS-AA was designed to be compatible with OPLS-UA,<sup>14</sup> the OPLS-AA/Berger combination is fully consistent.<sup>30</sup> Consequently, the combination of OPLS-AA amino acid force field with the united-atom lipid parameters developed by Berger and co-workers<sup>31</sup> has been successfully employed to run simulations of membrane proteins.<sup>25,30,32,33</sup> The use of a united-atom force field has the great advantage of decreasing the number of computed pairwise interactions up to 60%, while no drawback has been reported compared to all-atom parametrization. It has recently been described that Berger lipid parameters perform well together with the CHARMM22 protein force field.<sup>34</sup> In fact, AMBER, OPLS, CHARMM, and Berger force fields share

Received: July 14, 2011

Published: February 6, 2012

**Table 1.** Lennard-Jones Parameters  $\sigma$  (nm) and  $\epsilon$  (kJ/mol) and Atomic Partial Charges  $q$  for the Most Common Atom (or United-Atom) Types of (A) Proteins and Lipids, (B) Water, and (C)  $\text{Na}^+$  and  $\text{Cl}^-$  Ions

Part A												
atom(s)	AMBER99 <sup>a</sup>				OPLS-AA				BERGER			
	type	$\sigma$	$\epsilon$	$q^b$	type	$\sigma$	$\epsilon$	$q$	type	$\sigma$	$\epsilon$	$q$
O	O	0.296	0.879	−0.568	<i>opls_236</i>	0.296	0.879	−0.500	<i>LO</i>	0.296	0.879	−0.6/−0.7
O	O2	0.296	0.879	−0.800	<i>opls_441</i>	0.315	0.837	−0.920	<i>LOM</i>	0.296	0.879	−0.8
O	OS	0.300	0.711	−0.369	<i>opls_442</i>	0.290	0.586	−0.600	<i>LOS</i>	0.300	0.879	−0.8/−0.7
O	OH	0.307	0.880	−0.655	<i>opls_078</i>	0.307	0.711	−0.700				
N	N	0.325	0.711	−0.416	<i>opls_238</i>	0.325	0.711	−0.500				
N	N3	0.325	0.711	−0.385	<i>opls_103</i>	0.325	0.711	0	<i>LNL</i>	0.325	0.711	−0.5
S	SH	0.356	1.046	−0.312	<i>opls_083</i>	0.355	1.046	−0.450				
S	S	0.356	1.046	−0.108	<i>opls_084</i>	0.355	1.046	−0.470				
P	P	0.374	0.837	1.166	<i>opls_440</i>	0.374	0.837	1.620	<i>LP</i>	0.374	0.837	1.7
H	H	0.107	0.066	0.272	<i>opls_241</i>	0	0	0.300				
H	HC	0.265	0.066	0.060	<i>opls_140</i>	0.250	0.126	0.060				
H	HO	0.000	0	0.428	<i>opls_154</i>	0.312	0.711	−0.683				
C	C	0.340	0.356	0.597	<i>opls_235</i>	0.375	0.439	0.500	<i>LC</i>	0.375	0.440	0.7/0.8
C	CT	0.340	0.458	−0.183	<i>opls_135</i>	0.350	0.276	−0.180				
CH					<i>opls_006</i>	0.380	0.335	0.200	<i>LH1</i>	0.380	0.335	0.0/0.3
CH <sub>2</sub>					<i>opls_110</i>	0.380	0.494	0.250	<i>LH2</i>	0.391	0.494	0.3
CH <sub>2</sub>					<i>opls_071</i>	0.391	0.494	0	<i>LC2</i>	0.380	0.494	0.4/0.5
CH <sub>2</sub>									<i>LP2</i>	0.396	0.381	0
CH <sub>3</sub>					<i>opls_107</i>	0.396	0.607	0.250	<i>LC3</i>	0.396	0.607	0.4
CH <sub>3</sub>									<i>LP3</i>	0.396	0.569	0

Part B						
atom(s)	TIP3P			SPC		
	$\sigma$	$\epsilon$	$q$	$\sigma$	$\epsilon$	$q$
O	0.315	0.636	−0.834	0.315	0.649	−0.820
H	0	0	0.417	0	0	0.410

Part C						
atom	Joung <sup>64</sup> (AMBER)			Åqvist <sup>63</sup> (OPLS)		
	$\sigma$	$\epsilon$	$q$	$\sigma$	$\epsilon$	$q$
$\text{Na}^+$	0.244	0.366	1	0.333	0.012	1
$\text{Cl}^-$	0.448	0.149	−1	0.442	0.493	−1

<sup>a</sup>AMBER94, AMBER99, and AMBER03 have identical LJ parameters (see Methods section). <sup>b</sup>Charges are adopted from residues containing this atom type.

the same potential energy function, the only difference being the scaling factors for 1–4 interactions. Combining any of these protein force fields with Berger parameters of lipids thus requires either scaling 1–4 interactions independently<sup>35</sup> or refit the torsional potentials.<sup>36,37</sup>

In this paper, we asked whether the AMBER/Berger combination of force fields could be a better alternative to the previously validated OPLS-AA/Berger combination.<sup>30</sup> Two main arguments support their compatibility: (i) the functional form of nonbonded terms in AMBER and OPLS-AA equations are the same, and (ii) many nonbonded parameters in AMBER were originally adapted from OPLS-AA (Table 1). Thus, we assessed the performance of the AMBER99SB, AMBER03, and OPLS-AA force fields in combination with Berger parameter of lipids. Free energies of hydration, free energies of solvation in cyclohexane, and free energies of water to cyclohexane transfer were computed for neutral side-chain amino acids employing a cyclohexane model constructed from lipid methylene groups,<sup>37,38</sup> to quantitatively validate these force fields against experimental thermodynamic data. In addition, we tested the validity of our AMBER/Berger combination in the simulation of three diverse proteins: two  $\alpha$ -helical (the  $\beta_2$  adrenergic

receptor and aquaporin AQP1) and one  $\beta$ -barrel proteins. This was done by comparing the relative performance of AMBER99SB and OPLS-AA as protein force fields and of TIP3P and SPC water models.<sup>39,40</sup> Our results showed that AMBER99 force field was the most reliable in reproducing the experimental thermodynamic data. Also, AMBER99/Berger combination worked better than OPLS-AA/Berger in reproducing secondary structural properties of membrane proteins, whereas the choice of the water did not appear to be critical.

## METHODS

**Force Fields.** Force fields for the amino acids were OPLS-AA, AMBER99SB, or AMBER03 as implemented in GROMACS.<sup>9,14,41</sup> Topology files for palmitoyl-oleoyl phosphatidylcholine (POPC), using Berger parameters,<sup>31</sup> were based on files available at <http://moose.bio.ucalgary.ca/> that include optimized torsion potentials in the vicinity of the double bond.<sup>42</sup> Cyclohexane parameters were taken as in POPC methylene groups.<sup>37,38</sup> Combination rules and scaling factors for 1–4 interactions within OPLS-AA, AMBER, and Berger lipids were kept faithful to their original implementation. Thus, LJ  $\epsilon_{ij}$  parameters were always the geometric average of  $\epsilon_{ii}$

**Table 2.** Solvation Free Energies in Water (kJ/mol) for All Side-Chain Amino Acid Analogues, Except Pro and Gly, Computed with the OPLS/TIP3P, AMBER99/TIP3P, or AMBER03/TIP3P Force Fields<sup>a</sup>

residue	expt <sup>67</sup> $\Delta G$	OPLS/TIP3P			AMBER99/TIP3P			AMBER03/TIP3P		
		$\Delta G$	statistical error	absolute error	$\Delta G$	statistical error	absolute error	$\Delta G$	statistical error	absolute error
Asn	-40.5	-35.7	1.0	4.8	-38.9	1.8	1.6	-29.2	1.2	11.3
Gln	-39.2	-36.4	1.1	2.8	-39.3	1.7	-0.1	-46.8	1.2	-7.6
His	-42.1	-29.0	0.7	13.1	-37.1	1.3	5.0	-22.2	0.8	19.9
Asp	-27.5	-33.3	0.6	-5.8	-28.6	0.6	-1.1	-23.3	0.6	4.2
Ser	-21.2	-19.6	0.7	1.6	-19.3	0.7	1.9	-19.9	0.6	1.3
Glu	-26.6	-22.0	0.6	4.6	-28.3	0.7	-1.7	-25.8	0.7	0.8
Thr	-20.4	-18.4	0.9	2.0	-17.5	0.9	2.9	-15.8	0.6	4.6
Lys	-18.0	-8.3	2.0	9.7	-22.9	1.4	-4.9	-23.0	1.5	-5.0
Tyr	-25.6	-22.2	1.0	3.4	-18.8	1.2	6.8	-7.8	1.0	17.8
Cys	-5.2	-1.1	1.0	4.1	-0.8	2.1	4.4	0.7	1.7	5.9
Ala	10.1	9.1	0.6	-1.0	10.4	0.4	0.3	9.7	0.4	-0.4
Trp	-24.6	-19.2	1.0	5.4	-20.1	1.9	4.5	-14.3	1.2	10.3
Met	-6.2	-1.2	0.9	5.0	1.7	0.6	7.9	2.0	0.9	8.2
Phe	-3.2	-3.6	0.7	-0.4	-2.2	0.7	1.0	1.2	1.0	4.4
Val	8.4	9.9	0.8	1.5	9.9	0.4	1.5	9.5	0.5	1.1
Ile	9.0	10.0	0.9	1.0	10.2	0.7	1.2	11.3	0.8	2.3
Leu	9.5	9.7	0.8	0.2	10.6	1.1	1.1	9.4	0.8	-0.1
av error			0.9	+3.1		1.1	+1.9		0.9	+4.6

<sup>a</sup>Statistical errors were estimated using block averaging.<sup>38</sup> Absolute errors were calculated as the difference between computed and experimental values (adapted from ref 67).

and  $\epsilon_{ij}$ , whereas  $\sigma_{ij}$  parameters were computed either as the geometric (OPLS-AA and Berger lipids) or arithmetic (AMBER) average of  $\sigma_{ii}$  and  $\sigma_{jj}$ . 1–4 scaling factors for LJ and Coulombic interactions were 0.5 and 0.833 in AMBER, 0.5 and 0.5 in OPLS-AA, and 0.125 and 1.0 on the headgroup atoms of Berger lipids, respectively.<sup>24</sup> This 1–4 scaling was achieved using an explicit list of rescaled 1–4 pair interactions for the lipid head-groups, using a similar stratagem to that of Neal and collaborators.<sup>33</sup> This led to numerically equivalent energy terms either in the context of AMBER or OPLS-AA force fields without the need of any correction in the parameters.<sup>37</sup> A comparison between the main LJ parameters and partial charges of the main atom types in all force fields is displayed in Table 1. All simulations were performed with the GROMACS 4.5.3 simulation package.<sup>43</sup>

**Free Energy Calculations.** Free energies of solvation (i) in water, (ii) in cyclohexane, and (iii) of water to cyclohexane transfer were computed by thermodynamic integration procedures for 17 neutral side-chain amino acid analogues excluding Pro, Gly (lacks side-chain atoms), and Arg (the neutral analogue is not part of the AMBER force fields). The hydrogen atoms capping the side-chains were assigned the same charge as  $\beta$ -hydrogens, and the charge on the  $\beta$ -carbon was varied to achieve neutrality.<sup>38,44–46</sup> The fact that backbone atoms are not included in the model systems makes AMBER94<sup>47</sup> and the whole series of AMBER99 force fields and variants<sup>41,47–49</sup> identical since they only differ in the parametrization of backbone torsions. Cyclohexane molecules were initially in the chair conformation, and no interchange to the boat conformer was observed, in agreement with previous reports.<sup>50</sup>

Simulation systems consisted of a single amino acid analogue in a  $4.5 \times 4.5 \times 4.5$  nm<sup>3</sup> box, containing  $\sim 3000$  TIP3P<sup>39</sup> water molecules or  $\sim 500$  cyclohexane molecules. The simulations were conducted at constant isotropic pressure of 0.1 MPa with a time constant of 0.5 ps.<sup>51</sup> Integration of equations of motion

was performed using stochastic dynamics with a time-step of 2 fs. Temperature was kept at 298 K with a friction coefficient of 1 ps<sup>-1</sup> for the Langevin thermostat. All bonds involving hydrogen atoms were constrained using the LINCS algorithm.<sup>52</sup> The geometry of water molecules was fixed with the SETTLE algorithm.<sup>53</sup> The particle mesh Ewald method (PME) was used for electrostatic calculations with a grid spacing of 0.15 nm in all directions.<sup>54</sup> The real-space and neighbor search cutoff were set to 1.0 nm. LJ interactions were switched to zero between 0.8 and 0.9 nm. A long-range dispersion correction was applied to energy and pressure. The interactions between the amino acid analogues and the solvent were turned off with the use of a coupling parameter  $\lambda$ . A series of 43 windows with the  $\lambda$ -values equally spaced between 0 and 1 were conducted for the aqueous systems. For cyclohexane systems and simulations *in vacuo*, 29 windows were sufficient.<sup>55</sup> Each window was 550 ps long (50 ps of equilibration +500 ps of production). To avoid singularities, a soft core potential was used with  $\alpha = 0.6$ ,  $\sigma = 0.26$  nm, and a  $\lambda$ -power of 1. The choice of this setup was based on extensive literature in the field.<sup>38,44–46,55</sup> Even though a two-step procedure for decoupling electrostatic and LJ interactions independently has been shown to be slightly more efficient for water simulations,<sup>44</sup> the one-step procedure allowed easier comparison to previous results.

**Membrane Protein Simulations.** The crystal structures of  $\beta_2$ -adrenergic receptor (PDB ID: 2RH1<sup>56</sup>), the aquaporin 1 water channel (1J4N<sup>57</sup>), and the outer membrane porin protein 32 (2FGR<sup>58</sup>) were used as membrane model proteins. A single monomer was simulated in each case, corresponding to the first chain in the PDB. Titratable residues were modeled according to their protonation state in water at pH 7. Glu122 in  $\beta_2$ -adrenergic was modeled in the protonated state due to its orientation toward the lipid bilayer, and because Fourier-transform infrared experiments on the analogously positioned Glu122 of rhodopsin suggest its protonation.<sup>59</sup> Moreover,

**Table 3. Solvation Free Energies in Cyclohexane (kJ/mol) for All Side-Chain Amino Acid Analogues, Except Pro and Gly, Computed with the OPLS, AMBER99, or AMBER03 Force Fields<sup>a</sup>**

residue	expt <sup>69</sup> $\Delta G$	OPLS/TIP3P			AMBER99/TIP3P			AMBER03/TIP3P		
		$\Delta G$	statistical error	absolute error	$\Delta G$	statistical error	absolute error	$\Delta G$	statistical error	absolute error
Asn	-12.6	-12.8	0.6	-0.2	-12.2	0.4	0.4	-12.1	0.5	0.5
Gln	-15.8	-16.4	0.6	-0.6	-15.8	0.6	0.0	-16.4	0.5	-0.6
His	-23.4	-19.4	0.6	4.0	-19.8	0.5	3.6	-20.9	0.5	2.5
Asp	-9.2	-12.9	0.5	-3.7	-12.2	0.6	-3.0	-11.3	0.6	-2.1
Ser	-6.9	-4.3	0.5	2.6	-4.9	0.6	2.0	-4.6	0.4	2.3
Glu	-13.9	-16.0	0.8	-2.1	-16.1	0.5	-2.2	-15.8	0.5	-1.9
Thr	-9.5	-7.6	0.4	1.9	-8.9	0.4	0.6	-8.7	0.5	0.8
Lys	-16.4	-13.5	0.7	2.9	-16.9	1.0	-0.5	-16.7	0.9	-0.3
Tyr	-24.6	-22.4	0.6	2.2	-23.7	0.8	0.9	-23.0	0.7	1.6
Cys	-10.3	-8.3	0.3	2.0	-5.5	0.5	4.8	-6.8	0.4	3.5
Ala	0.6	-0.9	0.3	-1.5	-0.1	0.5	-0.7	-0.3	0.3	-0.9
Trp	-33.8	-29.6	0.6	4.2	-29.0	0.7	4.8	-30.0	1.2	3.8
Met	-15.8	-15.8	0.5	0.0	-13.2	0.8	2.6	-14.0	0.7	1.8
Phe	-17.5	-20.7	1.0	-3.2	-19.5	0.6	-2.0	-18.9	0.5	-1.4
Val	-8.5	-8.2	0.6	0.3	-8.6	0.6	-0.1	-8.3	0.4	0.2
Ile	-11.4	-12.5	0.5	-1.1	-13.0	0.7	-1.6	-13.3	0.8	-1.9
Leu	-10.9	-11.6	0.8	-0.7	-11.5	0.7	-0.6	-12.2	0.5	-1.3
av error			0.6	+0.4		0.6	+0.5		0.6	+0.4

<sup>a</sup>The cyclohexane parameters are based on Berger parameters for lipids (see Methods section). Statistical errors were estimated using block averaging.<sup>38</sup> Absolute errors were calculated as the difference between computed and experimental values (adapted from ref 69).

**Table 4. Free Energies (kJ/mol) of Water to Cyclohexane Transfer for All Side-Chain Amino Acid Analogues, Except Pro and Gly, Computed with the OPLS, AMBER99, or AMBER03 Force Fields<sup>a</sup>**

residue	expt <sup>69</sup> $\Delta G$	OPLS/TIP3P			AMBER99/TIP3P			AMBER03/TIP3P		
		$\Delta G$	statistical error	absolute error	$\Delta G$	statistical error	absolute error	$\Delta G$	statistical error	absolute error
Asn	-27.7	-22.9	1.2	4.8	-26.7	1.9	1.0	-17.1	1.3	10.6
Gln	-22.9	-19.9	1.3	3.0	-23.5	1.8	-0.6	-30.4	1.3	-7.5
His	-18.7	-9.6	0.9	9.1	-17.3	1.4	1.4	-1.3	1.0	17.4
Asp	-18.6	-20.4	0.8	-1.8	-16.4	0.8	2.2	-12.0	0.9	6.6
Ser	-14.2	-15.3	0.9	-1.1	-14.4	0.9	-0.2	-15.3	0.7	-1.1
Glu	-13	-6.0	1.0	7.0	-12.2	0.8	0.8	-10	0.8	3.0
Thr	-11.1	-10.8	1.0	0.3	-8.6	1.0	2.5	-7.1	0.8	4.0
Lys	-1.6	5.2	2.1	6.8	-6.0	1.6	-4.4	-6.3	1.6	-4.7
Tyr	-0.8	0.2	1.1	1.0	4.9	1.4	5.7	15.2	1.2	16
Cys	5.2	7.2	1.0	2.0	4.7	4.0	-0.5	7.5	1.7	2.3
Ala	7.7	10.0	0.7	2.3	10.5	0.6	2.8	10.0	0.5	2.3
Trp	9.5	10.4	1.2	0.9	8.9	2.0	-0.6	15.7	1.7	6.2
Met	9.7	14.6	1.0	4.9	14.9	1.0	5.2	16	1.2	6.3
Phe	14.1	17.1	1.2	3.0	17.3	0.9	3.2	20.1	1.1	6.0
Val	16.7	18.1	1.0	1.4	18.5	0.7	1.8	17.8	0.7	1.1
Ile	20.2	22.5	1.0	2.3	23.2	0.8	3.0	24.6	0.9	4.4
Leu	20.5	21.3	1.1	0.8	22.1	1.3	1.6	21.6	0.9	1.1
av error			1.1	+2.7		1.4	+1.5		1.1	+4.4

<sup>a</sup>Water parameters are TIP3P while cyclohexane parameters are based on Berger parameters for lipids (see Methods section). Statistical errors were estimated using block averaging.<sup>38</sup> Absolute errors were calculated as the difference between computed and experimental values (adapted from ref 69).

previously performed microsecond-time-scale MD simulations of the  $\beta_2$ -adrenergic receptor also consider Glu122 in its protonated state.<sup>60,61</sup>

Each protein was inserted in a pre-equilibrated box containing a POPC lipid bilayer, water, and a 0.15 M concentration of Na<sup>+</sup> and Cl<sup>-</sup> ions employing a previously described procedure.<sup>8,25</sup> For the  $\beta_2$ -adrenergic receptor, four different simulations were performed using AMBER99SB or

OPLS-AA force fields and TIP3P<sup>39</sup> or SPC<sup>40</sup> water molecules (see Table 1, part B). In contrast, aquaporin and the porin protein were simulated using AMBER99SB or OPLS-AA force fields and the TIP3P water model. None of the systems contained any ligand as its parametrization could be itself a potential source of variations that would difficult the comparison between force fields. It is important to outline that the conversion of ANTECHAMBER generated ligand



**Table 5.** Analysis of the Molecular Dynamics Simulations of the  $\beta_2$ -Adrenergic Receptor ( $\beta_2$ AR), the Aquaporin 1 Water Channel (AQP1), and the Outer Membrane Porin Protein 32 (Omp32), Embedded in a POPC Lipid Bilayer, with AMBER99SB or OPLS-AA Force Fields and TIP3P ( $\beta_2$ AR, AQP1, Omp32) or SPC ( $\beta_2$ AR) Water Molecules<sup>a</sup>

force field		rmsd C $\alpha$ (Å)	helical or $\beta$ -sheet <sup>a</sup>	MC–MC	$i \rightarrow i+3$	$i \rightarrow i+4$	$i \rightarrow i+5$	MC–SC
$\beta_2$ AR								
X-ray			230	190	19	159	5	34
OPLS/TIP3P	mean	3.25	209.7	156.5	39.3	108.8	4.4	41.5
	SD	0.26	9.7	6.3	4.3	5.6	0.8	3.1
OPLS/SPC	mean	2.85	208.8	154.4	41.3	106.1	4.3	39.9
	SD	0.25	11.3	6.3	4.4	5.7	1.0	3.2
AMBER/TIP3P	mean	1.94	229.7	185.5	23.3	154.4	4.2	38.4
	SD	0.19	7.1	5.6	3.6	5.6	1.0	3.0
AMBER/SPC	mean	2.03	226.9	187.7	25.8	152.8	4.6	37.9
	SD	0.17	8.0	5.6	3.6	5.4	0.9	3.1
AQP1								
X-ray			155	154	23	123	3	44
OPLS/TIP3P	mean	3.47	137.0	112.3	23.9	77.8	5.3	40.0
	SD	0.27	8.0	5.1	3.4	4.5	0.8	3.0
AMBER/TIP3P	mean	2.51	149.0	136.5	19.9	107.3	3.8	45.0
	SD	0.21	8.0	4.6	3.0	4.4	1.0	4.0
Omp32								
X-ray			187	201	24	9	1	167
OPLS/TIP3P	mean	1.92	181.1	182.4	14.2	8.0	0.9	159.3
	SD	0.11	3.5	4.3	1.9	1.1	0.5	0.9
AMBER/TIP3P	mean	1.40	187.0	192.6	22.7	6.7	1.4	161.7
	SD	0.07	3.8	4.1	2.2	1.3	0.6	0.1

<sup>a</sup>Several key features were analyzed: root mean square deviations (rmsd) on protein  $\alpha$ -carbons; number of main chain–main chain (MC–MC) hydrogen bonds between the N–H groups in the backbone of one  $\beta$ -strand and the C=O groups in the backbone of the adjacent  $\beta$ -strand in Omp32 simulations or between the carbonyl oxygen of residue  $i$  and the N–H atom of residue  $i+3$ ,  $i+4$ , or  $i+5$  in the helices forming  $\beta_2$ AR and AQP1; the number of main chain–side chain hydrogen bonds (MC–SC), and the number of residues forming either  $\beta$ -strands (Omp32) or  $\alpha$ -helices ( $\beta_2$ AR and AQP1). Mean values and standard deviations (SDs) are shown. Structures were collected for analysis every 15 ps during the last 50 ns of each simulation. The results are the average of two independent simulations (see Methods section). <sup>c</sup>Calculated with DSSP<sup>75</sup>

topologies to GROMACS is attainable by the amb2pdb.pl script (<http://ffamber.cnsmlb.edu/ffamber-tools.html>).<sup>62</sup> In all simulations, Berger lipid parameters were used.<sup>31</sup> Na<sup>+</sup> and Cl<sup>−</sup> ions parameters were from Åqvist<sup>63</sup> for OPLS-AA simulations and from Cheatham and co-workers<sup>64</sup> for AMBER simulations (see Table 1, part C). The different choice is obligatory considering critical effects of the different averaging of  $\sigma_{ij}$  parameters (see above) used in AMBER and in GROMACS regarding ion binding to phosphatidylcholine bilayers.<sup>65</sup>

Model systems were energy minimized and subsequently subjected to a 1 ns MD equilibration, with positional restraints on protein coordinates, to remove possible voids present in protein/lipids or proteins/water interfaces. These restraints were released, and 100 ns MD trajectories were produced, with pressure kept at 0.1 MPa in the three coordinate directions by independent Berendsen barostats.<sup>51</sup> Temperature was maintained constant at 300 K using separate v-rescale thermostats for the protein, lipids, and solvent molecules.<sup>66</sup> All bonds and angles were frozen using the LINCS algorithm,<sup>53</sup> allowing the use of a 2.5 fs time-step. LJ interactions were computed using a cutoff of 1.0 nm, and the electrostatic interactions were treated using PME with the same real-space cutoff. For each simulation setup and system, two independent replicas of 100 ns each were simulated for better statistics, resulting in an overall production simulation time of 1600 ns. Structures were collected for analysis every 15 ps.

## RESULTS

**Comparison between AMBER, OPLS-AA, and Berger Force Fields.** In AMBER99, AMBER03, and OPLS-AA force fields, as in most classical force fields, the interactions between nonbonded atoms are described by combining a Coulombic term plus a LJ potential. The first term relies on atomic charges reproducing the electrostatic potentials (derived using different schemes in each case), whereas the second takes into account both dispersion and nuclear repulsion. Table 1 shows LJ parameters and partial charges for the most relevant atom types. It can be seen that these force fields have similar LJ parameters, reflecting the common origin of AMBER and OPLS-AA force fields. In particular, nitrogen, sulfur, phosphate, and most oxygen atoms have identical LJ parameters. The most notable differences lie in the value of the  $\epsilon$  parameter. In addition, partial atomic charges are also similar between these force fields, although there is a tendency toward being larger in OPLS-AA than in AMBER force fields. It is noteworthy that Berger parameters for the lipid tails have no charges; thus, lipid tail–protein interactions are reduced to the LJ term.

**Free Energies of Solvation in Water and Cyclohexane, and Free Energies of Water to Cyclohexane Transfer.** In order to assess the quality of the AMBER99, AMBER03, and OPLS-AA force fields, free energies of solvation in water and cyclohexane and of water-to-cyclohexane transfer were computed for most amino acids (see Methods section). All force fields reproduced free energies of solvation in water in agreement with previously obtained calculations<sup>38,45,55</sup> and experimental values (Table 2).<sup>67</sup> Average errors are +1.9 kJ/

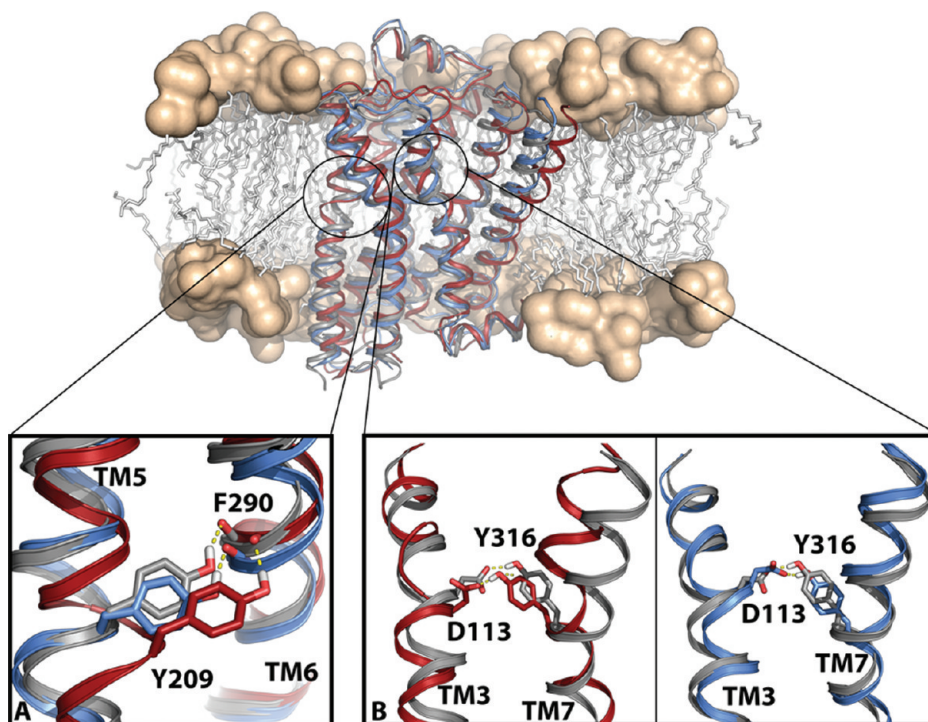


**Figure 1.** Comparison of the crystal structure of the  $\beta_2$ -adrenergic receptor (PDB id 2RH1 in gray) with two representative snapshots obtained from the AMBER99SB (blue) and OPLS-AA (red) molecular dynamics simulations of the receptor, embedded in a POPC lipid bilayer (lipid tails are shown as sticks, phosphate groups as surfaces, and TIP3P water molecules were omitted for clarity). Detailed view of (A) interhelical interactions involving the side chain of Y209<sup>TM5</sup> and the main chain carbonyl group of F290<sup>TM6</sup> and (B) the side-chain of D113<sup>TM3</sup> and the side-chain of Y316<sup>TM7</sup> (essential in maintaining the correct TM bundle conformation).

mol for AMBER99, +3.1 kJ/mol for OPLS-AA, and +4.6 kJ/mol for AMBER03 force fields (Table 2). The largest average error of the AMBER03 force field relies in the inaccurate prediction of the solvation free energy of Asn, His, Tyr, and Trp. This is due to the use of the new charge scheme introduced in AMBER03 force field paired with LJ parameters transferred from AMBER99. Fine-tuning of the parameters for the aromatic and hydroxyl groups of these amino acids overcomes this problem.<sup>68</sup> The use of AMBER99, AMBER03, or OPLS-AA force fields in the calculation of free energies of cyclohexane solvation give, in all cases, values that are all in excellent agreement with experimental measurements<sup>69</sup> (average errors of +0.4/0.5 kJ/mol, Table 3) and with previous free energy calculations.<sup>37,38</sup> The last computed free energy value, the water-to-cyclohexane transfer, is probably the most important since it estimates the lipophilicity of the amino acids. Average errors relative to experimental data are +1.5 kJ/mol for AMBER99, +2.7 kJ/mol for OPLS-AA, and +4.4 kJ/mol for AMBER03 force fields (Table 4). Clearly, the AMBER99 force field gave the smallest average error and, importantly, better reproduces the rank order of amino acid free energies. The AMBER03 force field fails in predicting the free energy transfers, mostly due to the incorrect prediction of the free energy of solvation in water (see above).

All these calculations support the reliability of the AMBER99/Berger combination of force fields, which properly describes the interactions of the amino acids with water, the hydrophobic cyclohexane solvent, and their relative preference for the hydrophilic water environment or the hydrophobic membrane core. Clearly, the quantitative agreement of the AMBER99/Berger combination of force fields with exper-

imental results surpasses the more extensively used OPLS-AA/Berger combination.

#### Simulations of Membrane Proteins in a Lipid Bilayer.

In order to further validate the use of the AMBER99SB/Berger combination of force fields, we conducted various simulations of the human  $\beta_2$ -adrenergic receptor ( $\beta_2$ AR),<sup>56</sup> the aquaporin 1 water channel (AQP1),<sup>57</sup> and the bacterial outer membrane porin protein 32 (Omp32)<sup>58</sup> in an explicit Berger-parametrized lipid bilayer. The helical bundle motif builds the three-dimensional structure of  $\beta_2$ AR and AQP1, whereas the  $\beta$ -barrel motif is observed in Omp32. Specifically,  $\beta_2$ AR, as other G protein-coupled receptors, is formed by seven transmembrane (TMs) domains,<sup>70</sup> AQP1 is composed by six TM domains plus two  $\alpha$ -helices that do not span the membrane, and Omp32 is formed by a 16-stranded  $\beta$ -barrel. MD simulations of  $\beta_2$ AR (with TIP3P and SPC water molecules), AQP1 (TIP3P), and Omp32 (TIP3P) were performed using AMBER99SB and OPLS-AA force fields (see Methods section). Table 5 summarizes key features aimed at analyzing the influence of the different setups in membrane and protein stability.

**Secondary/Tertiary Structure of the Protein.** The stability of the three-dimensional structure of  $\beta_2$ AR, AQP1, and Omp32 during the different simulations was monitored by root-mean-square deviations (rmsd). Average rmsd values on protein  $\alpha$ -carbons, relative to the protein crystal structure, are shown in Table 5. First, AMBER99SB/Berger combination of force fields reproduces lower rmsd values in all simulations as compared to the OPLS-AA/Berger combination. We can, thus, conclude that AMBER99SB/Berger better maintains the original structure of the protein than OPLS-AA/Berger, in agreement with previous results made on soluble peptides and proteins.<sup>71–74</sup> Second, rmsd values of the Omp32 simulations are lower than those of



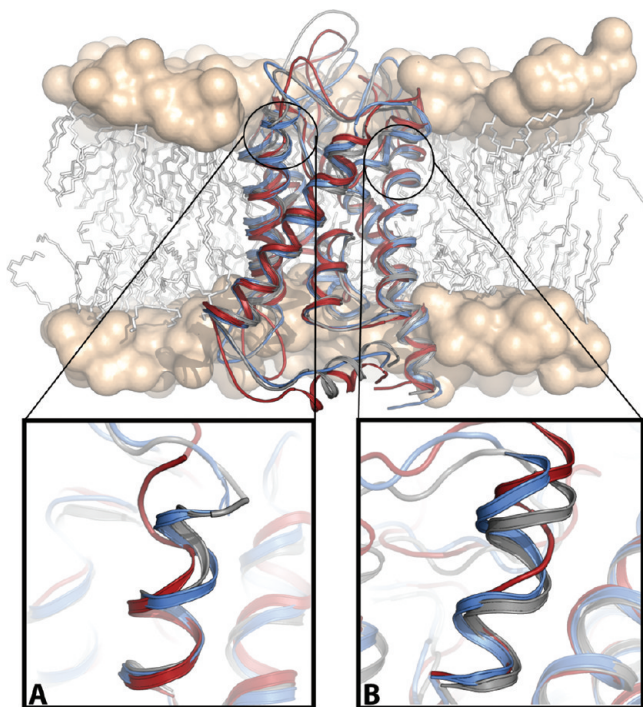


**Figure 2.** Comparison of the crystal structure of the aquaporin 1 water channel (PDB id 1J4N in gray) with two representative snapshots obtained from the AMBER99SB (blue) and OPLS-AA (red) molecular dynamics simulations of the protein, embedded in a POPC lipid bilayer (lipid tails are shown as sticks, phosphate groups as surfaces, and TIP3P water molecules were omitted for clarity). Insets are detailed views of specific parts of the protein to exemplify the instability of the helices in the OPLS-AA simulations.

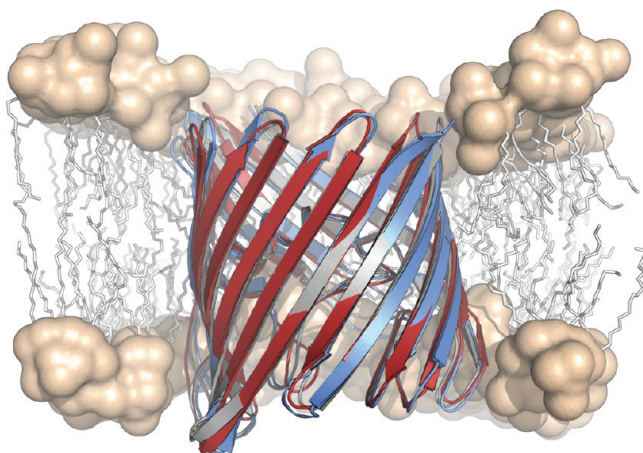


**Figure 3.** Comparison of the crystal structure of the outer membrane porin protein 32 (PDB id 2FGR in gray) with two representative snapshots obtained from the AMBER99SB (blue) and OPLS-AA (red) molecular dynamics simulations of the porin, embedded in a POPC lipid bilayer (lipid tails are shown as sticks, phosphate groups as surfaces, and TIP3P water molecules were omitted for clarity).

the  $\beta_2$ AR and AQP1 simulations. Thus, the  $\beta$ -barrel motif of Omp32 seems more stable than the helical bundle motif of  $\beta_2$ AR and AQP1. Also, third,  $\beta_2$ AR is more stable with the TIP3P water model than with SPC if the AMBER99SB force field is used, and the opposite (SPC better than TIP3P) with the OPLS-AA force field. This reflects that AMBER force fields were optimized for the TIP3P water model, whereas the OPLS-

AA force field was designed to be compatible with TIP3P, TIP4P, and SPC models.

A secondary structure analysis of the  $\beta_2$ AR, AQP1, and Omp32 simulations was performed using the Dictionary of Secondary Structure of Proteins (DSSP)<sup>75</sup> (Table 5). In the crystal structure of Omp32, 187 residues are forming the  $\beta$ -sheet secondary structure of the protein, which remains the same in the simulations with the AMBER99SB force field (187 residues) and slightly decreases with the OPLS-AA force field (181 residues). The stability of this  $\beta$ -sheet is basically achieved by a network of hydrogen bonds between the N–H groups in the backbone of one  $\beta$ -strand and the C=O groups in the backbone of the adjacent  $\beta$ -strand. Thus, we also monitored the total number of main-chain (MC)–MC hydrogen bonds during the simulations (Table 5). Clearly, the OPLS-AA force field (182 hydrogen bonds) decreases the average number of MC–MC hydrogen bonds more than the AMBER99SB force field (193 hydrogen bonds), relative to the initial structure (201 hydrogen bonds).

$\beta_2$ -AR and AQP1, which are mainly formed by TM helices that assemble together to form a bundle that spans the membrane, contain 230 and 155 helical residues, respectively. This number of helical residues of  $\beta_2$ -AR (230 residues) remains essentially the same in the simulations with the AMBER99SB force field (230 or 229 residues using TIP3P and SPC water models, respectively) and significantly decreases with the OPLS-AA force field (210 or 209 residues using TIP3P and SPC, respectively). Similarly, the 155 helical residues of AQP1 slightly decrease in the simulations with the AMBER99SB force field (149 residues) and significantly decrease with the OPLS-AA force field (137 residues). The stability of these  $\alpha$ -helices is basically achieved by the hydrogen bonds between the carbonyl oxygen of residue  $i$  to the N–H atoms of residue  $i + 4$ . Occasionally,  $\alpha$ -helices contain irregularities in the form of tight helical turns, characterized by  $i \rightarrow i + 3$  hydrogen bonds, or  $\pi$ -bulges, characterized by  $i \rightarrow i + 5$  hydrogen bonds. Thus, the total number of MC–MC hydrogen bonds was also used to study the stability of the helices during the simulations (Table 5). Compared to the initial  $\beta_2$ -AR structure (190 hydrogen bonds), the average number of hydrogen bonds remains almost unaltered with the AMBER99SB force field (186 or 188 for TIP3P and SPC) and decreases with the OPLS-AA force field (156 or 154 for TIP3P and SPC). Analogously, simulations of AQP1 with the AMBER99SB force field (137 hydrogen bonds) better maintain the average number of MC–MC hydrogen bonds than the OPLS-AA force field (112 hydrogen bonds), relative to the initial structure (154 hydrogen bonds). This clearly reflects the instability of the helices in the OPLS-AA simulations. A more detailed analysis shows that in all simulations the average number of  $i \rightarrow i + 4$  hydrogen bonds was smaller than in the initial crystal structure, with this effect being very remarkable in the simulations with the OPLS-AA force field (see Table 5). For instance, in simulations of  $\beta_2$ -AR, a significant number of the initial  $i \rightarrow i + 4$  hydrogen bonds moved to  $i \rightarrow i + 3$  type, a phenomenon often associated to the beginning of unfolding events in  $\alpha$ -helices. TM helices regularly contain distortions localized in regions with kinks, wide and narrow turns, or other noncanonical elements, and are energetically stabilized through complementary intra- and interhelical interactions involving polar side-chains (SCs), backbone carbonyls, and, in some cases, specific functional water molecules embedded in the TM bundle.<sup>76</sup> Thus, the number of MC–SC hydrogen bonds was

Table 6. Coulombic, Lennard-Jones (LJ), and Total Energy Terms for Protein–Lipid and Protein–Water Interactions in Molecular Dynamics Simulations of the  $\beta_2$ -Adrenergic Receptor ( $\beta_2$ AR), the Aquaporin 1 Water Channel (AQP1), and the Outer Membrane Porin Protein 32 (Omp32), Embedded in a POPC Lipid Bilayer, with AMBER99SB or OPLS-AA force fields and TIP3P ( $\beta_2$ AR, AQP1, Omp32) or SPC ( $\beta_2$ AR) Water Molecules<sup>a</sup>

force field		E(protein–lipid)			E(protein–water)			membrane thickness
		Coulombic	LJ	total	Coulombic	LJ	total	
β <sub>2</sub> AR								
OPLS/TIP3P	mean	−1897	−3552	−5449	−13 321	−867	−14 189	2.87
	SD	197	87	283	386	119	505	0.03
OPLS/SPC	mean	−1940	−3597	−5537	−13 627	−856	−14 483	2.84
	SD	128	116	244	349	124	473	0.03
AMBER/TIP3P	mean	−1416	−3791	−5206	−12 720	−1047	−13 766	3.03
	SD	131	98	229	343	107	450	0.03
AMBER/SPC	mean	−1626	−3647	−5273	−12 844	−1206	−14 050	2.98
	SD	131	92	223	340	111	451	0.03
AQP1								
OPLS/TIP3P	mean	−1572	−2873	−4445	−9280	−850	−10 130	2.92
	SD	151	88	239	372	106	478	0.03
AMBER/TIP3P	mean	−1445	−2989	−4434	−9105	−920	−10 025	3.02
	SD	140	88	228	354	96	450	0.03
Omp32								
OPLS/TIP3P	mean	−2172	−3148	−5320	−16 431	−767	−17 198	2.83
	SD	213	87	301	400	133	533	0.03
AMBER/TIP3P	mean	−1811	−3314	−5124	−16 380	−1095	−17 475	2.94
	SD	166	88	254	399	124	523	0.03

<sup>a</sup>Mean values and standard deviations (SDs) are shown. Membrane thickness is measured as the average distance between the two planes defined by the first aliphatic atom of the lipids. All values were computed by averaging the last 50 ns of two independent simulations.

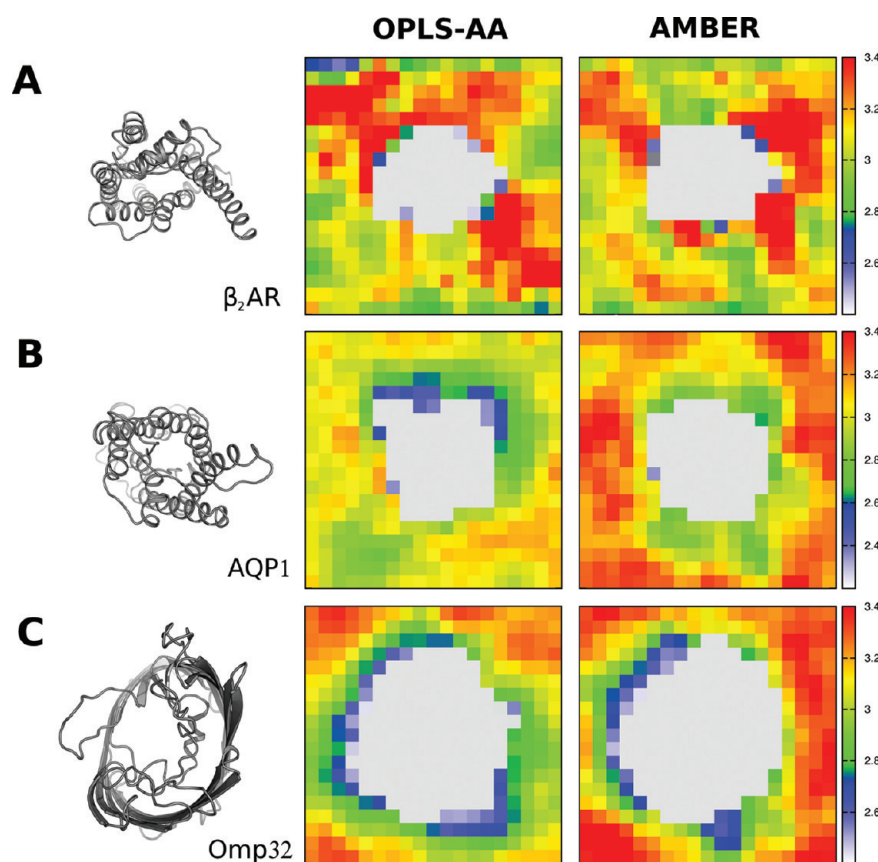


Figure 4. Membrane thickness measured as the average distance between the two planes defined by the first aliphatic atom of the lipids in a  $20 \times 20$  grid. Each square represents the average membrane thickness computed for all lipids located in this area. All values were computed by averaging the last 50 ns of two independent simulations.



also monitored during the simulations (Table 5). There is an increase in the average number of MC–SC hydrogen bonds (larger for OPLS-AA than for AMBER) in  $\beta_2$ AR simulations.

Figures 1 ( $\beta_2$ AR), 2 (APQ1), and 3 (Omp32) show the superimposition of the crystal structure (gray) with two representative snapshots from the AMBER99SB (blue) and OPLS-AA (red) simulations. The larger stability of the  $\beta$ -barrel motif of Omp32 compared to the helical bundle motif of  $\beta_2$ AR and AQP1 (see above) is also displayed in these superimpositions, in which the structure of Omp32 remains almost unchanged during the simulations. In contrast, comparison of the helices forming the structure of  $\beta_2$ AR and APQ1 shows much larger deviations. Insets in Figures 1 and 2 show that the helical secondary structures obtained in the simulations with the OPLS-AA force field more significantly deviate from their respective crystal structure than those obtained with the AMBER99SB force field. In particular, insets in Figure 2 exemplify the instability of the helices in the OPLS-AA simulations, while insets in Figure 1 illustrate representative examples of MC–SC and SC–SC hydrogen bonds. Inset A in Figure 1 shows the interhelical interaction between the SC of Y209<sup>TM5</sup> and the MC carbonyl group of F290<sup>TM6</sup>. The OPLS-AA force field, in contrast to AMBER99SB, induces a movement of Y209<sup>TM5</sup> that alters the secondary structure of TM 5. Inset B shows another type of interhelical interactions, between the SC of D113<sup>TM3</sup> and the SC Y316<sup>TM7</sup>. Similarly, this SC–SC hydrogen bond alters, in OPLS-AA force field, the secondary structure of TM 7 relative to the initial structure. Thus, the decrease of intrahelical MC–MC hydrogen bonds (destabilization of the TM helices) observed with the OPLS-AA force field might have its origin in the over stabilization of MC–SC and SC–SC hydrogen bonds.

**Membrane Thickness.** In all simulations membrane bulk properties are in agreement with experimental measurements as well as with previous simulations of membrane proteins embedded in a lipid bilayer.<sup>77–81</sup> Membrane thickness (measured as the average distance between the two planes defined by the first aliphatic atom of the lipids) is in the range between 2.83 and 3.03 nm (see Table 6). These small differences indicate that influence of protein/lipid force fields on membrane thickness is small. Importantly, we have shown before that the ion parameters/water model used has a deeper influence on membrane thickness than protein/lipid force fields.<sup>82–84</sup> Membrane thickness varies depending on whether the lipid is interacting with the protein or not. Thickness profiles in an area located around the protein show no significant differences between the simulations with the AMBER99SB and OPLS-AA force fields (Figure 4). According to the Orientations of Proteins in Membranes (OPM) database,<sup>85</sup> hydrophobic thickness ranges between 3.0 and 3.5 nm in G protein coupled receptors, 2.8–3.2 nm in aquaporins, and ~2.5 nm in Omp porins, in good agreement with these computed maps.

**Protein–Lipid and Protein–Water Interactions.** Table 6 shows the average energy terms for protein–lipid and protein–water interactions. The Coulombic energy term is systematically less negative in AMBER99SB than in OPLS-AA force field (reflecting the different partial charges), whereas the LJ energy term is the opposite, more negative in AMBER99SB than in OPLS-AA (reflecting the different  $\sigma_{ij}$  parameter for  $i$ – $j$  atom pairs). Notably, total energies (Coulombic + LJ) are similar in all simulation setups, thus permitting us to conclude that

protein–lipid (differences are <5%) and protein–water (<3%) interactions are not very sensitive to force field choice.

## CONCLUSIONS

Finding a biomolecular force field for membrane protein simulations that combines a correct description of protein secondary structure, easy ligand parametrization, and a good membrane description is not a trivial task. In the present work we have tested whether AMBER99 force field for the protein domain could be combined with Berger parameters for the lipid part, as an alternative choice to the previously validated and widely used OPLS-AA/Berger combination. In order to validate the reliability of this AMBER99/Berger combination, free energies of solvation in water and in cyclohexane and of water-to-cyclohexane transfer for amino acid side-chain analogues were computed for two versions of the AMBER force fields (AMBER99 and AMBER03) and for OPLS-AA. Comparison of the results with experimental data shows that AMBER99SB and Berger parameters are fully compatible, and their combination gives even slightly more accurate free energies than those obtained using the OPLS-AA/Berger combination. Even more interesting are the results of MD simulations of all three membrane-proteins we used to test our system: the  $\beta_2$ -adrenergic receptor, the aquaporin 1 water channel, and the outer membrane porin protein 32. In all cases the AMBER99/Berger combination provides, relative to OPLS-AA/Berger, a better description of main chain–main chain interactions, which finally leads to a better description of the protein secondary/tertiary structure. Because the GAFF AMBER force field in combination with the ANTECHAMBER suite of programs makes ligand parametrization an easy task, the AMBER99/Berger combination is also a reliable and a strong choice for the simulations of membrane proteins in complex with synthetic ligands.

## AUTHOR INFORMATION

### Corresponding Author

\*E-mail: arnau.cordomi@uab.cat. Phone: (+34) 935813812. Fax: (+34) 93 581 2344.

### Notes

The authors declare no competing financial interest.

## ACKNOWLEDGMENTS

This work was supported by grants from MICINN (SAF2010-22198-C02-02), and ISCIII (RD07/0067/0008). A.C. is a recipient of a contract grant from ISCIII.

## REFERENCES

- (1) Karplus, M. *Biopolymers* **2003**, 68, 350.
- (2) Karplus, M. *Acc. Chem. Res.* **2002**, 35, 321.
- (3) Hopkins, A. L.; Groom, C. R. *Nat. Rev. Drug Discovery* **2002**, 1, 727.
- (4) Tusnady, G. E.; Dosztanyi, Z.; Simon, I. *Bioinformatics* **2004**, 20, 2964.
- (5) White, S. H. *Protein Sci.* **2004**, 13, 1948.
- (6) Etchebest, C.; Debret, G. *Methods Mol. Biol.* **2010**, 654, 363.
- (7) Ash, W. L.; Zlotmisl, M. R.; Oloo, E. O.; Tieleman, D. P. *Biochim. Biophys. Acta* **2004**, 1666, 158.
- (8) Cordomi, A.; Edholm, O.; Perez, J. J. *J. Comput. Chem.* **2007**, 28, 1017.
- (9) Duan, Y.; Wu, C.; Chowdhury, S.; Lee, M. C.; Xiong, G.; Zhang, W.; Yang, R.; Cieplak, P.; Luo, R.; Lee, T.; Caldwell, J.; Wang, J.; Kollman, P. J. *Comput. Chem.* **2003**, 24, 1999.

- (10) Wang, J. M.; Cieplak, P.; Kollman, P. A. *J. Comput. Chem.* **2000**, *21*, 1049.
- (11) MacKerell, A. D.; Bashford, D.; Bellott, M.; Dunbrack, R. L.; Evanseck, J. D.; Field, M. J.; Fischer, S.; Gao, J.; Guo, H.; Ha, S.; Joseph-McCarthy, D.; Kuchnir, L.; Kucera, K.; Lau, F. T. K.; Mattos, C.; Michnick, S.; Ngo, T.; Nguyen, D. T.; Prodhom, B.; Reiher, W. E.; Roux, B.; Schlenkrich, M.; Smith, J. C.; Stote, R.; Straub, J.; Watanabe, M.; Wiorkiewicz-Kuczera, J.; Yin, D.; Karplus, M. *J. Phys. Chem. B* **1998**, *102*, 3586.
- (12) Feller, S. E.; MacKerell, A. D. *J. Phys. Chem. B* **2000**, *104*, 7510.
- (13) Jorgensen, W. L.; Tiradorives, J. *J. Am. Chem. Soc.* **1988**, *110*, 1657.
- (14) Jorgensen, W. L.; Maxwell, D. S.; TiradoRives, J. *J. Am. Chem. Soc.* **1996**, *118*, 11225.
- (15) Van Gunsteren, W. F.; Berendsen, H. J. C. *Groningen Molecular Simulation (GROMOS) Library Manual*, BIOMOS b.v.; University of Groningen: Groningen, 1987.
- (16) Wang, J.; Wolf, R. M.; Caldwell, J. W.; Kollman, P. A.; Case, D. A. *J. Comput. Chem.* **2004**, *25*, 1157.
- (17) Case, D. A.; Cheatham, T. E.; Darden, T.; Gohlke, H.; Luo, R.; Merz, K. M.; Onufriev, A.; Simmerling, C.; Wang, B.; Woods, R. J. *J. Comput. Chem.* **2005**, *26*, 1668.
- (18) Tessier, M. B.; DeMarco, M. L.; Yongye, A. B.; Woods, R. J. *Mol. Simul.* **2008**, *34*, 349.
- (19) Sonne, J.; Jensen, M. O.; Hansen, F. Y.; Hemmingsen, L.; Peters, G. H. *Biophys. J.* **2007**, *92*, 4157.
- (20) Rosso, L.; Gould, I. R. *J. Comput. Chem.* **2008**, *29*, 24.
- (21) Jojart, B.; Martinek, T. A. *J. Comput. Chem.* **2007**, *28*, 2051.
- (22) Siu, S. W.; Vacha, R.; Jungwirth, P.; Bockmann, R. A. *J. Chem. Phys.* **2008**, *128*, 125103.
- (23) Kukol, A. *J. Chem. Theory Comput.* **2009**, *5*, 615.
- (24) Lindahl, E.; Edholm, O. *Biophys. J.* **2000**, *79*, 426.
- (25) Cordoní, A.; Perez, J. J. *J. Phys. Chem. B* **2007**, *111*, 7052.
- (26) Hofsäss, C.; Lindahl, E.; Edholm, O. *Biophys. J.* **2003**, *84*, 2192.
- (27) Böckmann, R. A.; Grubmüller, H. *Angew. Chem., Int. Ed.* **2004**, *43*, 1021.
- (28) Kandasamy, S. K.; Larson, R. G. *Biophys. J.* **2006**, *90*, 2326.
- (29) Essex, J. W.; Hann, M. M.; Richards, W. G. *Philos. Trans. R. Soc., B* **1994**, *344*, 239.
- (30) Monticelli, L.; Simoes, C.; Belvisi, L.; Colombo, G. *J. Phys.: Condens. Matter* **2006**, *18*, S329.
- (31) Berger, O.; Edholm, O.; Jähnig, F. *Biophys. J.* **1997**, *72*, 2002.
- (32) Provasi, D.; Bortolato, A.; Filizola, M. *Biochemistry* **2009**, *48*, 10020.
- (33) Chakrabarti, N.; Neale, C.; Payandeh, J.; Pai, E. F.; Pomes, R. *Biophys. J.* **2010**, *98*, 784.
- (34) Sapay, N.; Tieleman, D. P. *J. Comput. Chem.* **2011**, *32*, 1400.
- (35) Neale, C.; Pomès, P. Combination rules for united-atom lipids and OPLSAA proteins. <http://www.pomeslab.com/files/lipidCombinationRules.pdf>.
- (36) Ulmschneider, J. P.; Ulmschneider, M. B. *J. Chem. Theory Comput.* **2009**, *5*, 1803.
- (37) Tieleman, D. P.; MacCallum, J. L.; Ash, W. L.; Kandt, C.; Xu, Z. T.; Monticelli, L. *J. Phys.: Condens. Matter* **2006**, *18*, S1221.
- (38) MacCallum, J. L.; Tieleman, D. P. *J. Comput. Chem.* **2003**, *24*, 1930.
- (39) Jorgensen, W. L.; Chandrasekhar, J.; Madura, J. D.; Impey, R. W.; Klein, M. L. *J. Chem. Phys.* **1983**, *79*, 926.
- (40) Berendsen, H. J. C.; Grigera, J. R.; Straatsma, T. P. *J. Phys. Chem.* **1987**, *91*, 6269.
- (41) Sorin, E. J.; Pande, V. S. *Biophys. J.* **2005**, *88*, 2472.
- (42) Bachar, M.; Brunelle, P.; Tieleman, D. P.; Rauk, A. *J. Phys. Chem. B* **2004**, *108*, 7170.
- (43) Hess, B.; Kutzner, C.; van der Spoel, D.; Lindahl, E. *J. Chem. Theory Comput.* **2008**, *4*, 435.
- (44) Steinbrecher, T.; Mobley, D. L.; Case, D. A. *J. Chem. Phys.* **2007**, *127*, 214108.
- (45) Shirts, M. R.; Pande, V. S. *J. Chem. Phys.* **2005**, *122*, 134508.
- (46) Shirts, M. R.; Pitera, J. W.; Swope, W. C.; Pande, V. S. *J. Chem. Phys.* **2003**, *119*, 5740.
- (47) Cornell, W. D.; Cieplak, P.; Bayly, C. I.; Gould, I. R.; Merz, K. M.; Ferguson, D. M.; Spellmeyer, D. C.; Fox, T.; Caldwell, J. W.; Kollman, P. A. *J. Am. Chem. Soc.* **1995**, *117*, 5179.
- (48) Gnanakaran, S.; Garcia, A. E. *Proteins* **2005**, *59*, 773.
- (49) Hornak, V.; Abel, R.; Okur, A.; Strockbine, B.; Roitberg, A.; Simmerling, C. *Proteins* **2006**, *65*, 712.
- (50) Raschke, T. M.; Levitt, M. *J. Phys. Chem. B* **2004**, *108*, 13492.
- (51) Berendsen, H. J. C.; Postma, J. P. M.; DiNola, A.; Haak, J. R. *J. Chem. Phys.* **1984**, *81*, 3684.
- (52) Hess, B.; Bekker, H.; Berendsen, H. J. C.; Fraaije, J. G. E. M. *J. Comput. Chem.* **1997**, *18*, 1463.
- (53) Miyamoto, S.; Kollman, P. A. *J. Comput. Chem.* **1992**, *13*, 952.
- (54) Darden, T.; York, D.; Pedersen, L. *J. Chem. Phys.* **1993**, *98*, 10089.
- (55) Hess, B.; van der Vegt, N. F. J. *J. Phys. Chem. B* **2006**, *110*, 17616.
- (56) Cherezov, V.; Rosenbaum, D. M.; Hanson, M. A.; Rasmussen, S. G.; Thian, F. S.; Kobilka, T. S.; Choi, H. J.; Kuhn, P.; Weis, W. I.; Kobilka, B. K.; Stevens, R. C. *Science* **2007**, *318*, 1253–1254.
- (57) Sui, H.; Han, B. G.; Lee, J. K.; Walian, P.; Jap, B. K. *Nature* **2001**, *414*, 872.
- (58) Zachariae, U.; Kluhspies, T.; De, S.; Engelhardt, H.; Zeth, K. *J. Biol. Chem.* **2006**, *281*, 7413.
- (59) Fahmy, K.; Jager, F.; Beck, M.; Zvyaga, T. A.; Sakmar, T. P.; Siebert, F. *Proc. Natl. Acad. Sci. U.S.A.* **1993**, *90*, 10206.
- (60) Dror, R. O.; Arlow, D. H.; Borhani, D. W.; Jensen, M. O.; Piana, S.; Shaw, D. E. *Proc. Natl. Acad. Sci. U.S.A.* **2009**, *106*, 4689.
- (61) Vanni, S.; Neri, M.; Tavernelli, I.; Rothlisberger, U. *Biochemistry* **2009**, *48*, 4789.
- (62) Mobley, D. L.; Chodera, J. D.; Dill, K. A. *J. Chem. Phys.* **2006**, *125*, 084902.
- (63) Åqvist, J. *J. Phys. Chem.* **1990**, *94*, 8021.
- (64) Joung, I. S.; Cheatham, T. E. III. *J. Phys. Chem. B* **2008**, *112*, 9020.
- (65) Cordoní, A.; Edholm, O.; Perez, J. J. *J. Chem. Theory Comput.* **2009**, *5*, 2125.
- (66) Bussi, G.; Zykova-Timan, T.; Parrinello, M. *J. Chem. Phys.* **2009**, *130*, 074101.
- (67) Wolfenden, R.; Andersson, L.; Cullis, P. M.; Southgate, C. C. *Biochemistry* **1981**, *20*, 849.
- (68) Yang, L.; Tan, C. H.; Hsieh, M. J.; Wang, J.; Duan, Y.; Cieplak, P.; Caldwell, J.; Kollman, P. A.; Luo, R. *J. Phys. Chem. B* **2006**, *110*, 13166.
- (69) Radzicka, A.; Wolfenden, R. *Biochemistry* **1988**, *27*, 1664.
- (70) Liapakis, G.; Cordoní, A.; Pardo, L. *Curr. Pharm. Des.* **2012**, *18*, 175.
- (71) Hu, Z.; Jiang, J. *J. Comput. Chem.* **2009**, *31*, 371–380.
- (72) Best, R. B.; Buchete, N. V.; Hummer, G. *Biophys. J.* **2008**, *95*, L07.
- (73) Yoda, T.; Sugita, Y.; Okamoto, Y. *Chem. Phys.* **2004**, *307*, 269.
- (74) Yoda, T.; Sugita, Y.; Okamoto, Y. *Chem. Phys. Lett.* **2004**, *386*, 460.
- (75) Kabsch, W.; Sander, C. *Biopolymers* **1983**, *22*, 2577.
- (76) Pardo, L.; Deupi, X.; Dolker, N.; Lopez-Rodriguez, M. L.; Campillo, M. *ChemBioChem* **2007**, *8*, 19.
- (77) Hyslop, P. A.; Morel, B.; Sauerheber, R. D. *Biochemistry* **1990**, *29*, 1025.
- (78) Kucerka, N.; Tristram-Nagle, S.; Nagle, J. F. *J. Membr. Biol.* **2005**, *208*, 193.
- (79) König, B.; Dietrich, U.; Klose, G. *Langmuir* **1997**, *13*, 525.
- (80) Smaby, J. M.; Momsen, M. M.; Brockman, H. L.; Brown, R. E. *Biophys. J.* **1997**, *73*, 1492.
- (81) Lantzh, G.; Binder, H.; Heerklotz, H.; Wendling, M.; Klose, G. *Biophys. Chem.* **1996**, *58*, 289.
- (82) Gurtovenko, A. A.; Vattulainen, I. *J. Phys. Chem. B* **2008**, *112*, 1953.
- (83) Böckmann, R. A.; Hac, A.; Heimburg, T.; Grubmüller, H. *Biophys. J.* **2003**, *85*, 1647.

(84) Cordoní, A.; Edholm, O.; Perez, J. J. *J. Phys. Chem. B* **2008**, *112*, 1397.

(85) Lomize, M. A.; Lomize, A. L.; Pogozheva, I. D.; Mosberg, H. I. *Bioinformatics* **2006**, *22*, 623.